J. Cosmet. Sci., **60,** 57–83 (January/February 2009)

Papers Presented at the 2008 Annual Scientific Meeting and Technology Showcase (Thursday's Program)

December 11–12, 2008
New York Hilton
New York, NY

SPECIFIC FILAGGRIN INDUCER PRYIDOXINE AND ITS DERIVATIVE: EFFECTS ON CULTURED HUMAN KERATINOCYTES AND HUMAN INTACT SKIN

Hitoshi Masaki, Ph.D., Miyuki Fujishiro, Syoichi Yahagi and Yuri Okano, Ph.D.

Nikkol Group Cosmos Technical Center, 3-24-3, Itabashi-ku, Tokyo 174-0046, Japan

Objectives

Pyridoxine (VB6) plays an essential role in the maintenance of homeostasis by supporting protein synthesis as well as amino acid and lipid metabolism. A lack of VB6 leads to several kinds of diseases in the skin, including pellagra-like dermatitis (1) and dermatitis seborrheica (2). It has been reported that the topical application of VB6 could improve the symptoms of the aforementioned diseases (3) and also that it is beneficial to use VB6-therapy for atopic dermatitis (4). Despite many clinical observations, however, the precise mechanism of VB6 on skin is less well-known. Nevertheless, the facts suggest that VB6 does indeed have an impact on the terminal differentiation process in the epidermis.

The aim of this study is to address the physiological effects of VB6 on the skin and to develop a feasible derivative of VB6 that both maintains the properties of VB6 as well as remains stable in formulations. To accomplish this, we synthesized vitamin B6 tri-isopalmitate (VB6-IP) and evaluated the effects by comparing it with VB6.

Materials and Methods

Cell culture: Keratinocytes were treated with KG2 (without bovine pituitary gland extract (BPE)) medium (KURABO) containing various concentrations of samples.

RT-PCR: Total RNA was extracted from keratinocytes, which were treated with samples for 48 hours using Trizol reagent (Invitrogen) following the instructions. cDNA was synthesized using Superscript II (Invitrogen), and PCR was performed using Taq polymerase (Rosh) in an automated thermal cycler (Trio thermoblock 48, Biometra) to identifiy the marker genes of epidermal terminal differentiation such as profilaggrin, serine permitoyl transferase (SPT), involucrin, keration10.

Dot-blotting: *Proteins were extracted from keratinocytes which were treated with various concentrations of samples for 72 hr, by 0.5% Triton X-100 (Wako) in PBS (-) with 2mM phenylmethylsulfonyl fluoride (PMSF) (SIGMA). The protein was blotted on nitrocellulose membranes (BIO-RAD). Afterwards, immunoblotting was sequentially performed using two types of antibodies, anti-human filaggrin specific antibody (1st antibody, ARGENE) and HISTOFINE simple stain PO(M) (2nd antibody, Nichirei). A chemiluminescence was visualized using a Lumi-Light Western Blotting Substrate (Roche).*

Immunohistochemical staining: *VB6 (1.5 mM) or VB6-IP (1.5 mM) was topically applied to RSE (TOYOBO). After 1 week of cultivation, the frozen cross-sections of the RSE were stained with Anti-human filaggrin specific antibody (ARGENE) and FITC-labeled mouse anti-IgG (ZYMED Laboratories). The staining of filaggrin was observed under a fluorescence microscope.*

Human test: *The effects on skin moisture of a gel formulation containing 3% VB6-IP and its placebo gel formulation were evaluated using the sprit face method. Both gels were applied to a human volunteer (n=10) twice a day. After 7, 14, 28 day-application, the water content was estimated by measuring skin-surface conductance using SKICON-200EX (IBS). The protocol had been approved by the ethical committee of Cosmos technical center and all volunteers provided a written consent form.*

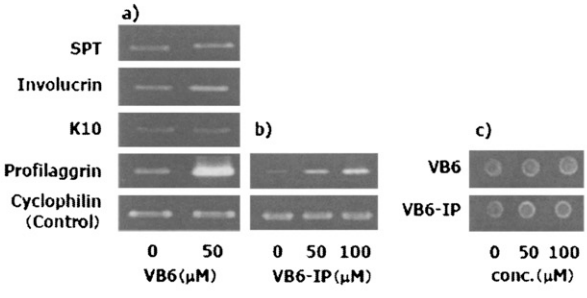

Fig.1 Effects of VB6 and VB6-IP on the terminal differentiation marker proteins. a) mRNA expression by VB6, b) mRNA expression VB6-IP, c) filaggrin protein by VB6 and VB6-IP.

Results

Effect of VB6 on specific markers on terminal differentiation: We examined the effect of VB6 on the expression of specific markers related to the terminal differentiation of keratinocytes. In the RT-PCR analysis, contrary to our expectations, VB6 up-regulated profilaggrin mRNA expression exclusively, thus not working on SPT, involucrin, and K10 expressions (Fig. 1a). Also, in dot-blotting analysis, we found that VB6 treatment of keratinocytes accelerated filaggrin protein expression (Fig. 1b).

Characterization of a new VB6-derivative, VB6-IP: To investigate whether VB6-IP maintains a function similar to VB6, we evaluated the effect of VB6-IP on the expression/production of filaggrin. As shown in Fig. 1c, VB6-IP significantly increased filaggrin expression/production.

Filaggrin production in RSE: *Since VB6-IP shows an oil-soluble property, it was expected that VB6-IP would have a more beneficial effect on the skin than VB6 would. VB6-IP showed much more stimulation of filaggrin in RSE than VB6 showed (Fig. 2).*

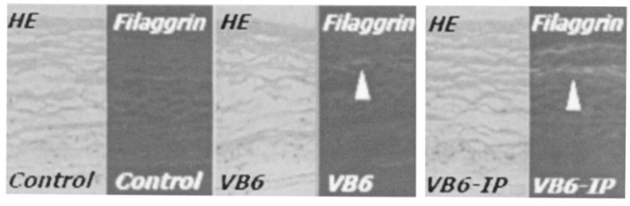

Fig. 2 Effect of VB6 and VB6-IP on filaggrin production in reconstructed skin equivalents (RSE). **HE: hematoxylin-eosin staining Fillaggrin: immunostainig**

Skin moisturization test (human): Finally, we carried out human tests to address the potential of VB6-IP on intact human skin. When compared with the results using the placebo gel, the results using the VB6-IP gel showed that the water content in the skin dramatically increased over the 28 days after application (Data not shown).

Conclusion

In this study, we examined the critical role that VB6 plays in epidermal functioning by focusing on the differentiation process of epidermal keratinocytes. VB6 provided a specific up-regulation of profilaggrin mRNA/protein in keratinocytes. This up-regulation makes VB6 a good candidate for skin moisturizing agents in a new category of moisturizers in which moisturization is achieved through the enhancement of NMF regulation. In addition, we found that VB6-IP greatly accelerates filaggrin production and improves the water contact of the skin surface.

References

1. GYÖRGY P., *Nature.*, **133**, 498-4999 (1934).
2. Schereiner, A.W., et al., *J. Lab. Clin. Med.*, **40**, 121-130 (1952).
3. Effersoe, H., *Acta. Derm. Venereol.*, **34**, 272-278 (1954)
4. Balabolkin II,et al., *Vopr. Med. Khim.*, **38**, 36-40 (1992)

CONFOCAL RAMAN SPECTROSCOPY OF ACTIVE PERMEATION INTO STRATUM CORNEUM FROM LAMELLAR LIPID FORMULATIONS

David J. Moore, Ph.D., Xiaohong Bi, Donald Koelmel and Mihaela Gorcea

International Specialty Products, Corporate Research Center, Wayne, NJ
djmoore@ispcorp.com

Keywords: confocal Raman, delivery, lamellar lipids, permeation, stratum corneum

Introduction

In recent years both infrared and Raman microscopy have been utilized to investigate molecular structure and composition of biomedical tissues, including skin. These techniques are particularly powerful as they can provide direct molecular information on the distribution and molecular structure of sample constituents. Confocal Raman spectroscopy possesses additional benefits as a non-invasive method that provides depth-resolved information at a high spatial resolution (up to 1-2 um along the axial). The recent development and application of this technique in skin research has permitted the non-destructive *in vivo* and *ex vivo* characterization of skin constitutes such as natural moisturizing factor, water and lipids [1-4]. More recently, confocal Raman spectroscopy of *ex vivo* skin has been utilized to determine the chemical stability and concentration profile of topically applied exogenous molecules as well as their interaction with endogenous molecules [5, 6]. Very recent studies have used confocal Raman spectroscopy as a method to monitor *in situ* both pro-drug and drug permeation and metabolism in the skin [7].

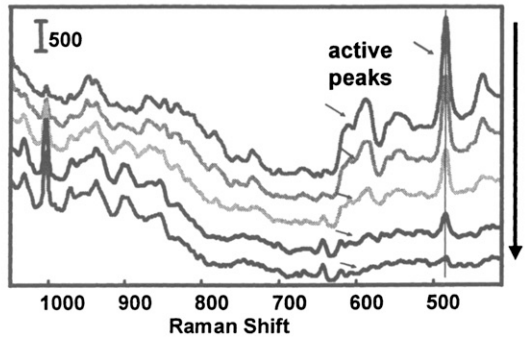

Methods

This presentation will describe new studies of active permeation into the stratum corneum of full thickness skin utilizing confocal Raman spectroscopy. Specifically, active delivery and permeation from topical lamellar lipid gel formulations containing 1-2 % level of cosmetic actives (for example salicylic acid, arbutin or tocopheryl phosphate) has been non-invasively and quantitatively measured using confocal Raman. In parallel, active delivery from these lipid lamellar gel formulations has been determined by the traditional, but more destructive, measurement of sequential tape stripping.

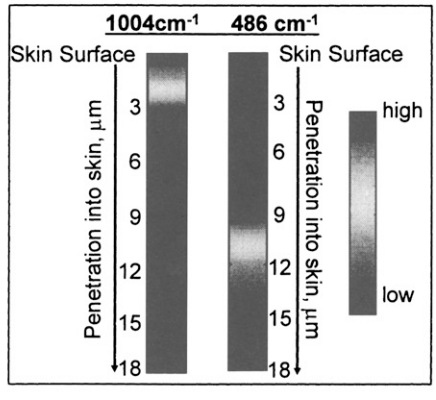

Results and Discussion

Data from both experimental approaches will be discussed focusing on the depth profile and quantitative amount of active permeation as a function of skin temperature and application time. The data show that active concentration and location in the skin can be non-invasively and quantitatively monitored with confocal Raman spectroscopy.

A specific advantage of the confocal Raman approach to measuring skin delivery is the potential to monitor the chemical stability of an active as it penetrates into the skin. This is very important information for actives that are delivered in a "pro-" form and require subsequent chemical modification to become active (as in our recent study of 5FU – see [7]). However, such molecular understanding is equally valuable when molecular conversion is not desired. Thus, in addition to the confocal Raman data showing stratum corneum penetration of tocopheryl phosphate, data will be presented illustrating that this molecule is not degraded, or chemically converted in the stratum corneum from its biologically active phosphorylated form.

Conclusion

In summary, this presentation will discuss both measurement approaches and demonstrate how they can be used in a complementary manner to quantitatively measure the effective delivery of cosmetic actives into stratum corneum when topically applied at levels of ~1-2 %.in lamellar lipid gel formulations. Furthermore, the confocal Raman measurement is shown that the active is chemically stable and does not undergo unwanted chemical conversion in the skin.

References:

[1] Caspers PJ, Lucassen GW, Wolthuis R, Bruining HA, Puppels GJ, In vitro and in vivo Raman spectroscopy of human skin. *Biospectroscopy*, 4:S31-S39 (1998)
[2] Caspers PJ, Lucassen GW, Carter EA, Bruining HA, Puppels GJ, In vivo confocal Raman microspectroscopy of the skin: Noninvasive determination of molecular concentration profiles. *J Invest Dermatol,* 116:434-441
[3] Caspers PJ, Lucassen GW, Puppels GJ, Combined in vivo confocal Raman spectroscopy and cofocal microscopy of human skin. *Biophys J,* 85: 572-580, (2003)
[4] Xiao C, Flach CR, Marcott M, Mendelsohn R, Uncertainties in depth determination and comparison of multivariate with univariate analysis in confocal Raman studies of a laminated polymer and skin. *Appl Spectrosc*, 58: 382-289 (2004)
[5] Caspers PJ, Williams A.C., Carter EA, Edwards HG, Barry BW, Bruining HA, Puppels GJ, Monitoring the penetration enhancer dimethyl sulfoxide in human stratum corneum in vivo by confocal Raman spectroscopy, *Pharm Res*, 19: 1577-1580 (2002)
[6] Xiao C, Moore DJ, Rerek ME, Flach CR, Mendelsohn R, "Feasibility of Tracking Phospholipid Permeation into Skin Using Infrared and Raman Microscopic Imaging," *J.Invest.Dermatology*, 124: 622-632 (2005)
[7] Zhang G, Moore DJ, Sloan KB, Flach CR, Mendelsohn R, Imaging the prodrug-to-drug transformation of a 5-Fluorouracil derivative in skin by confocal Raman microscopy, *J.Invest.Dermatology*, 127:1205-1209 (2007)

MULTICULTURAL SKIN TECHNOLOGY

Zoe Diana Draelos, MD

Dermatology Consulting Services, High Point, NC

Beneath the stratum corneum and epidermis, skin is the same. The dermis appears a creamy white in persons of all cultural backgrounds, thus multicultural skin technology focuses primarily on the interaction between melanin production, melanin transfer, and factors affecting melanogenesis. Subtle differences in melanin allow skin to appear almost black when the concentration is high and a reddish-white when the concentration is low. Melanin is produced in two forms: pheomelanin, a polymer of benzothiazine which is red, and eumelanin, a polymer of dihydroxyindole, dihydroxyindole carboxylic acid, and their reduced forms, which is a dark brown. It is the various combinations of these two pigments that produce the diversity of skin colors observed in modern society. This presentation examines new understandings in multicultural skin technology.

Melanin Production

Melanin production is the primary differentiating factor in multicultural skin. Skin color is determined by several genes, including the recently discovered SLC24A5, which accounts for the average difference of 30 melanin units between European and African skin. Another important gene is the MCIR, also known as melanocortin-1-receptor, which is a hormone produced by the pituitary gland that stimulates melanin production. The MCIR gene consists of 954 nucleotides. Among Africans there are no differences in the amino acid sequences of the receptor proteins, but 18 differences were noted among light-skinned populations in Ireland, England, and Sweden. While it has been thought that light skin was a genetic mutation to allow adequate vitamin D production by the body, this theory has been questioned.

Melanin is produced in response to sun exposure, transforming harmful UV radiation into heat. This explains the uncomfortable skin warmth when dark skin is exposed to the sun, which is not the case with poorly melanized skin, accounting for the preponderance of light complected persons engaging in tanning practices. Tanning is response to skin injury and not health benefit.

Melanin Transfer

The number of melanocytes, typically 1000-2000/mm^2 of skin, does not differ between skin colors, but their ability to produce and transfer melanin is different. Melanocytes are located at the lower level of the epidermis transferring melanin to skin cells in packages known as melanosomes. Melanosomes in recipient cells accumulate atop the cellular nucleus, where they protect nuclear DNA from ionizing radiation damage and the resultant cellular mutations. These cellular mutations contribute to photoaging when mild, precancerous changes when moderate, and photocarcinogenesis when severe. Irregular melanin transfer results in mottled pigmentation characteristic of photoaged skin.

Factors Affecting Melanogenesis

Melanogenesis can be affected by many factors that differ cross culturally. Irregular melanin production is of prime cosmetic importance. Increased melanin production can occur in response to a variety of different stimuli, including UV radiation, injury, and hormone production. Melanogenesis can be epidermal or dermal. Epidermal melanogenesis is due to the release and subsequent oxidation of arachidonic acid to prostaglandins, leukotrienes, and other inflammatory mediators, which initiate pigment production. If the inflammation disrupts the basal cell layer, the melanin is released and trapped by macrophages in the dermis. Dermal pigment, also known as pigmentary incontinence, is not amenable to cosmetic intervention while epidermal pigment can be effectively modulated. The difference can be detected visually, since epidermal pigment can vary from light brown to dark black while dermal pigment has a grayish appearance.

Summary

New understandings in melanin production and transfer are key to evolving multicultural skin technology. Irregular pigmentation is a sign of aging and poor health in persons of all skin colors necessitating improvement by modulating the driving factors that induce melanogenesis.

FRONTIERS OF SCIENCE AWARD LECTURE SPONSORED BY COSMETICS AND TOILETRIES®

REBUILDING PEOPLE: THE COMING ERA OF TISSUE ENGINEERING

Buddy D. Ratner, Ph.D.

University of Washington Engineered Biomaterials (UWEB)
University of Washington, Seattle, WA 98195-5061

Tissue engineering uses ideas in biology, medicine and engineering to grow living tissues and organs for repair or replacement of aged, damaged and diseased tissues and organs. Tissue engineering is closely related to regenerative medicine and is often considered a fast path to early clinical successes in regenerative medicine. Successful tissue engineering demands collaboration between basic scientists, applied scientists, engineers, clinicians, and industry.

It is my opinion that tissue engineering will revolutionize medicine and cosmetic repair/enhancement in the next ten years. Specific applications that are now rapidly evolving include bladder, bone, skin, heart muscle, cornea and cartilage. Also applications in cosmetic surgery are being explored and include wrinkle fillers, breast augmentation, hair regeneration and plastic surgery implants.

How are tissues engineered? A basic scheme is illustrated below.

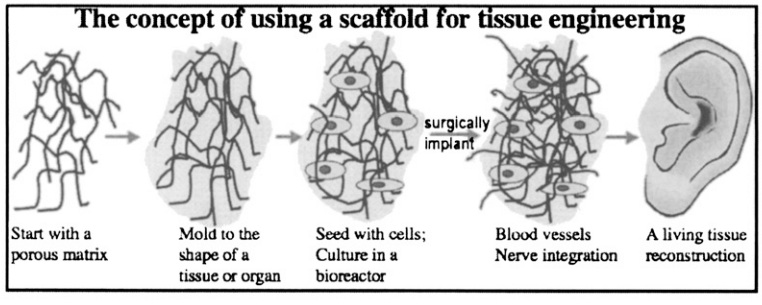

There are foundation ideas, technologies and concepts that underlie the engineering of all tissues. These foundations are:

Scaffolds: The scaffold permits cell attachment and growth and shapes the tissue. Scaffolds should biodegrade over an appropriate period of time so the tissue, as it forms, develops strength and functionality as the scaffold loses strength and dissolves into the organism. Scaffolds can be porous, fibrous or gel-like. They can be hard or soft and are sometimes injectable.

Bioreactors: Scaffolds seeded with cells can be "conditioned" in a bioreactor. By allowing the cells to accommodate to their scaffold environment, proliferate and start on the path to a tissue, one can use this *in vitro* initial step to speed and enhance *in vivo* outcomes. If the cells proliferate too exuberantly they will present a diffusion barrier preventing nutrients and oxygen from reaching cells in the core of the cell mass. These cells will die leaving a necrotic core.

Surgical integration: The scaffold + cells must be integrated with the patient. Upon implantation, the cell mass will not be connected to the patient's circulatory system. So a key issue is, how quickly can we generate new blood vessels to sustain the forming tissue?

Angiogenesis: Angiogenesis is the process of blood vessel formation. Many biological and non biological strategies can be used to stimulate blood vessel formation. One strategy involving engineered porous materials is described below.

Innervation: Along with blood vessels, nerves must grow into the new tissue to properly connect it to the body.

Appropriate biomechanics: Tissues and organs often serve a mechanical function. Blood vessels must be burst-resistant. Knee cartilage must survive heavy, cyclic loads. Heart muscle must be strong and coordinated. Sometimes, mechanical preconditioning in a bioreactor can lead to improved mechanical properties for the growing tissue.

Inflammation/healing: The tissue engineered construct must heal into the host and appropriately integrate. Healing must go down a reconstructive pathway, and not a fibrotic-necrotic pathway.

Cell sources: Where will the cells come from to make engineered tissues? Some adult cells retain good proliferative ability. A small biopsy from the patient can be expanded in culture to provide large numbers of cells. For difficult to proliferate cells, and situations where the replacement part must available immediately and "off-the shelf," two options are possible: (1) allogeneic cells (cells from one individual expanded up in a bioreactor and used for all implants) that can have immunologic consequences, and (2) embryonic stem cells differentiated into the cells types of interest.

Market realities: Issues here include sterilization, storage, regulatory concerns and business models.

The use of a novel scaffold for tissue engineering will be presented. A scaffold made by sphere-templating with pores that are uniform in size has been especially effective in inhibiting fibrosis, encouraging angiogenesis and reconstructing tissue. This type of scaffold may have exceptional value in cosmetic reconstructions. The discussion will focus particularly on skin and heart muscle, tissues where we have the most data at present. Other technologies used in conjunction with the scaffolds to achieve the objectives will be presented.

Acknowledgements

This work has been funded by a Biomedical Research Partnership grant from the National Heart, Lung and Blood Institute (the BEAT grant), and by an Engineering Research Center from the National Science Foundation (University of Washington Engineered Biomaterials, UWEB).

GLYCOKINES: SUGAR MOLECULES WITH SPECIFIC MESSENGER ACTIVITY IMPROVE TISSULAR COHESION AS MEASURED WITH A NOVEL, NON-INVASIVE, NON-TOUCH "ELASTICITY" TECHNOLOGY

Denise Gabriele, Philippe Mondon, Ph.D., Claire Mas Chamberlain and Karl Lintner, Ph.D.

Sederma, S.A.S., Le Perray en Yvelines, France

INTRODUCTION:

Any multicellular organism of sufficient size and complexity needs means of communication between different body parts, between organs and cells. This is achieved either by transmission of electric signals in nerve cells or by chemical signals released and transported. The latter mechanism involves many different types of molecules which are sometimes called hormones. After the discovery of steroid hormones in the early 20th century, and the peptide hormones in the second half of this epoch, many more signal molecules of different chemical nature have been found. It has been observed recently that certain oligosaccharides, fragments and analogs of natural polysaccharides may also possess this function of eliciting specific biochemical and biological reactions in skin cells, which thus represents a new category of possible skin care active ingredients.

OBJECTIVE OF THE STUDY:

It was thus the objective of our work to study and understand the mechanisms of action of small sugar molecules in eliciting biological responses in skin cells and to correlate their activity with *in vivo* results obtained with a novel, non-touch skin elasticity measurement technique.

METHODS:

The oligosaccharides are obtained by fermentation of *Rhizobium meliloti* and selective hydrolysis of the exopolysaccharide produced. Analytical characterization is under progress. *In vitro, ex vivo* and *in vivo* investigations were initiated. Cell culture studies with human fibroblasts (HF) allowed us to quantitatively evaluate elastin/tropoelastin synthesis by ELISA method or FTIC antibody tagging and image analysis after 15 days of incubation in DMEM. TGF-β was used as control. Stimulation of Laminins and hyaluronic acid synthesis was followed in a culture of human keratinocytes (HK), also by ELISA techniques. Clinical studies on 26 human volunteers employed a novel no-contact skin elasticity measurement device (fig. 1) ("Aeroflexmeter™") to observe cutaneous tissue cohesion. This device consists of a precisely mounted and positionable nozzle to send compressed air to the skin and of a laser beam to follow and record the deformation of the skin surface via CCD and appropriate computer software. A cream containing the oligosaccharides was tested against vehicle, with twice daily application for 2 months. In addition to the above described skin elasticity measurement, moisturisation, skin surface smoothness and cutaneous barrier (TEWL) were investigated by standard techniques. Statistical analysis tests were used to judge the results.

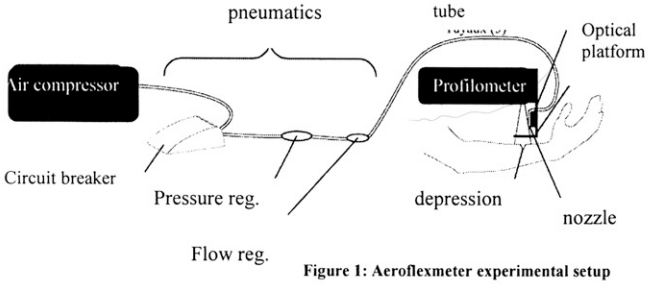

Figure 1: Aeroflexmeter experimental setup

RESULTS:

***in vitro* studies on human fibroblasts**: Incubation of fibroblasts with the oligosaccharides leads to stimulation of the synthesis of Elastin/Tropoelastin in fibroblasts. At the low concentration of 0.06% a strong response is observed with these molecules (+359% over baseline, $p<0.01$). It is important to note that the number of cells in the culture is not influenced by the addition of the saccharides. Although, as expected, for

TGFβ, a slight increase in cell number is observed (+24%), there is no proliferative effect with the test molecule, and the differences are due to selective, specific stimulation.

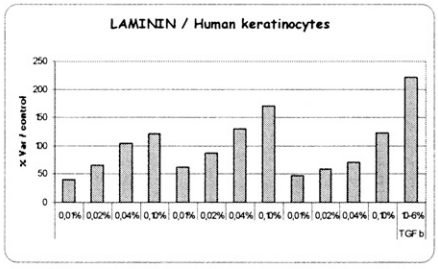

Fig. 2: stimulation of Laminin 5 synthesis in three separate runs as a function of concentration

***In vitro* studies on human keratinocytes**: Of particular interest are the studies on keratinocytes, in view of the fact that these cells are increasingly recognized as important players in skin physiology and condition. Three days of incubation of these cells in monolayer culture with the oligosaccharide lead to a strong, reproducible, significant ($p<0.01$) and concentration dependent synthesis of Laminins (Figure 2). Again, quantification (Hoechst coloration) of the number of cells in the culture after incubation shows the absence of a proliferative effect: the cell multiplication rate is NOT modified by the glycokines which indicates a specific stimulatory signal. These results were confirmed using skin explants. Increasing epidermal synthesis of Laminine 5 was observed with an oligosaccharide containing ointment (topical application).

***In vivo* (clinical) studies**: Skin moisturisation (Corneometer® and MoistureMeter-D®), skin surface profile (replicas), barrier integrity (TEWL) and skin elasticity parameters (Aeroflexmeter®) were studied. Moisturisation improved significantly (+28% vs. placebo; $p<0.02$) after 8 weeks of application of the test formula containing the oligosaccharides. Barrier repair afforded by the treatment with the product is shown by rapid decrease in TEWL values after insult and recovery; skin smoothness and corneocyte cohesion are increased significantly (Fig. **3**), whereas the vehicle cream had little effect of no significance.

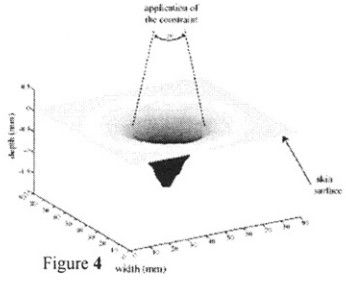

Figure **4**

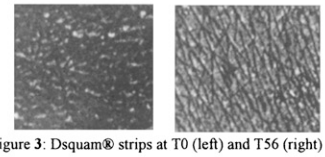

Figure **3**: Dsquam® strips at T0 (left) and T56 (right)

The novel no-contact elasticity measuring device allowed us to obtain images as shown in fig. **4** from which new parameters such as tissue cohesion (absorption of stress) and resilience can be extracted (fig. **5**). A parallel study on 65 persons of various age groups confirmed that these parameters correlate well ($r=0.6$) with age (to be published). The results of the treatment of the volunteers with the oligosaccharides confirm that, based on the skin's elasticity parameters, an "anti-age" effect can be obtained with the oligosaccharides.

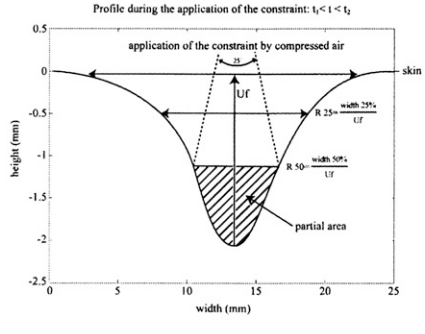

Figure **5**: novel skin elasticity parameters: R25: "resistance to deformation" ; A25: "absorption" of the impact = width 25%/width50%

CONCLUSION: In addition to classical "hormones" (steroids, peptides, bio-amines), it appears that small **specific** sugar molecules are also able to elicit specific biological responses from skin cells, at very low concentrations. They thus constitute an additional tool in the strive to repair damaged skin tissue. The complete set of data on cells *in vitro,* on skin *ex vivo* and on human panelists confirms the coherence of this approach. Furthermore, a new non-touch technique to measure skin elasticity parameters allows us to go beyond the Cutometer® in analyzing tissue cohesion non-invasively.

THE STUDY OF CELLULAR SENESCENCE IN VITRO: MODELS, PROTOCOLS AND MECHANISMS AND WAYS TO DELAY THE ONSET OF SENESCENCE IN VITRO

Karl Lintner, Ph.D., Philippe Mondon, Ph.D., and Francois Vissac

Sederma, S.A.S., Le Perray en Yvelines, France

Keywords :telomers, corticoids, accelerated ageing, DNA array, SIPS

INTRODUCTION:

The anti-aging market is booming. Claims of slowing down, stopping or even reversing the aging process can be found, more or less openly, in numerous advertisements. Even if clinical data substantiating these promises are rare [1], research into cellular aging processes (*in vitro*) is intense and quite sophisticated. Various techniques of Stress Induced Premature Senescence (SIPS) are used in this field.

OBJECTIVE:

To study the question: What does skin ageing mean at the cellular level? What are the mechanisms? Can the "senescence" be accelerated (for screening purposes) or delayed (for anti-age activity)? Which SIPS is most promising?

MATERIAL and METHODS:

Monolayer cell culture studies: Telomere measurements involved trypsinizing the fibroblast cell culture, extracting DNA and using Hinf1 and Rsa1 restriction enzymes to separate telomere sequences from the residual DNA. Agarose gel eletrophoreses followed by Southern Blot transfer and hybridization with TTAGGG-digoxigenine probes allows for antibody coupled alkaline phosphatase revelation and quantification of the luminescence via CCD camera or photography and scanning.

Life span: Normal human **fibroblasts** were cultured until their "twelfth mitosis". The cells were then divided into 2 groups (3 culture dishes each): a control group and a group incubated with 3μM of an antioxydant isoprenyl derivative (GGA) daily. Each dish containing DMEM medium with 10% FCS was inoculated with approximately 50,000 cells, and the cells cultured to confluence or until there were sufficient cells for 50,000 cells to be harvested for the next cycle. At each time point the cells were harvested by trypsinization, counted, and a 50,000-cell aliquot sub-cultured for the next cycle. The procedure was repeated until no further cell growth could be obtained.

DNA array: an "anti-ageing" ingredient was incubated with a human **keratinocyte** culture for 24 hours. The mRNA of the cells was extracted using a commercially available kit (Roche Kit V6 - Extraction of total RNA). In parallel, solvent controls were run and subjected to extraction in the same manner. The expression profile of the genes was determined using CodeLink Whole Genome chips for each sample of purified RNA which enables the analysis of the expression profile of the 45,000 human genes arrayed on the chip. *PredictSearch*® text and data mining software was used to analyse the gene activity.

ex vivo Studies on human skin explants in a survival medium. The model is based on the observation that human skin, maintained under carefully controlled conditions in a survival state close to living conditions (except for blood irrigation and nerve connections), can be artificially "aged" by incubation with a strong topically administrated hydrocortisone (2 days). The skin fragments of biopsies harvested from 8 different donors were maintained in diffusion-type cells with appropriate nutrient medium. The skins were treated topically for 2 days with Diprosone® cream, and with an 'anti-age' ingredient (also topically) in hydroglycolic solution for up to 14 days. End points investigated were the amount of Laminin 5 (immune detection and semiquantitative scoring) and Hyaluronic acid receptor CD 44 (a transmembrane glycoprotein) by the same method.

RESULTS and DISCUSSION:

Cells can be artificially "aged" by various means of SIPS (hydrogen peroxide treatment, UV irradiation, glucocorticoid treatment). Whereas adding H_2O_2 to a cell culture and observing the effects can be of interest to study radical scavenging efficacy of molecules, and UV irradiation of cells allows one to study DNA oxidation, dimer formation, and many other deleterious phenomena directly or indirectly connected to ageing, these insults do not represent true senescence of the cells. Hydrocortisones have been described as useful tools to induce SIPS. Their *in vivo* effects are well known as undesirable side symptoms of a medical treatment (e.g. eczema): skin atrophy, telangiectasy, stretch marks, skin thinning, reduced wound healing capacity etc. have been observed [1]. This can be reproduced in *ex vivo* studies on human skin biopsies from cosmetic surgery (fig. 1).

***ex vivo* study of the effects on human skin explants in a survival medium:**

The following pictures show the effect of cortisone application on the skin: Laminin 5, an all important protein at the epidermal/dermal junction (EDJ), is badly disorganized by this treatment (figure 1b). Treatment with a rather specific polysaccharide molecule fragment restores the quantity of laminin and the correct shape of the EDJ.

The pictures are representative of the 8 donors and visual scoring leads to significant quantitative results. The interesting aspect is that normal human keratinocytes in monolayer culture are also stimulated to synthesize laminin 5 when incubated with this ingredient. Furthermore, the same cells also increase the synthesis rate of hyaluronic acid, a fact which is then borne out in the same 8 donor skins by staining for the CD44 HA receptor protein (figures not shown). Finally, the DNA chip analysis reveals that the ingredient stimulates Vitronectine which is a protein central to the pathways of protein synthesis, tissue repair and cellular protection. Simultaneous stimulation of TGF-□, leading to Laminin 5 synthesis and EDJ repair rounds off the more coherent anti-age character of this approach.

Figure 1a (Laminin-5 is stained in red) Figure 1b figure 1c

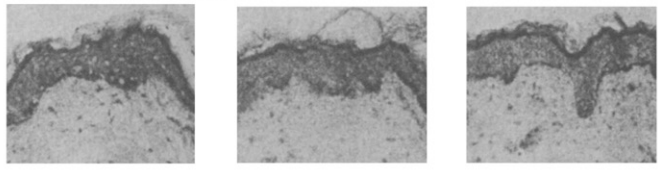

Control skin + dermocorticoïde + dermocorticoïde + PS

LIFE SPAN:

However, even this accelerated approach to senescence is only partly satisfying. True senescence can be observed, along with the markers, only after long term cell culture (6 months or more) and repeated passages (cf. the Hayflick model [2]). In this model, it is possible to observe the onset of cellular senescence when the cell multiplication rate drops sharply. Normal human fibroblasts can only divide a limited number of times *in vitro.* We observed that between cycle 12 (T0 for the study) and cycle 19 (T90 days), cell division slowed down equally in both cultures: the time needed to obtain approximately 200,000 cells increased from 7 to 18 days. However, after cycle 19, the situation evolved differently between control culture and the one exposed to an anti-age molecule:

For the control fibroblasts, a very clear "falloff" was observed (table I), giving rise to cultures that were unable to become confluent: replicative capacity was considerably reduced. The time necessary to generate 50,000 cells became increasingly long (77 days for cycle 25): senescence had become established.

The situation was markedly different for the cells exposed to an antioxidant, "anti-age" molecule at 3µM concentration. The fibroblasts retained their replicative capability until cycle 24 (115,000 cells). Replicative capability was thus retained longer than the controls (109,000 cells, cycle 20), and the differences were highly significant. This elaborate, albeit tedious, protocol nevertheless confirms that cellular senescence can be retarded with an appropriate molecule, such as a powerful antioxidant.

Table I: Replicative senescence of normal human fibroblasts in the presence or absence of 3µM GGA.(n=3)

Number of cells	Cycle 20 14 days	Cycle 21 22 days	Cycle 22 20 days	Cycle 24 28 days	Cycle 25 77 days
Time (months vs.T0)	≈3.5	≈4	≈5	≈7	9.5
Control	**109,000**	**94,000**	**67,000**	**64,000**	**52,000**
GGA 3µM	**145,000**	**154,000**	**157,000**	**115,000**	**95,000**
Significance	**p<0.05**	**p<0.01**	**p<0.01**	**p<0.01**	**p<0.01**

TELOMER LENGTHS:

Having observed in DNA array experiments that incubation of keratinocytes with the cited molecule led to stimulation of genetic activity tied to telomere protection and repair (e.g. CDK2 and CBX5/HP1 are jointly activated which are both involved in the machinery regulating and elongating telomeres, CBX5/HP1 procures the repeating nucleotide string, TTAGGG, of the telomere.), we attempted to confirm this activity on the telomers themselves. Figure 2 shows that ageing cells have shorter average telomere length, and a wider distribution of base pair numbers. This technique and approach will now allow us to quantify the potential anti-age effect on telomers of this – and other – molecules.

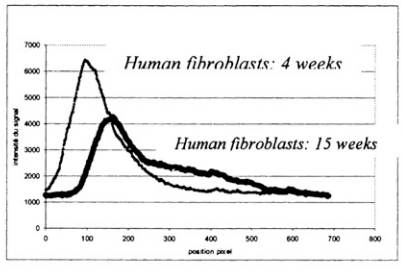

CONCLUSION: Although "accelerated cellular senescence" or SIPS (stress induced premature senescence) by culturing cells with peroxide or glucocorticoids or UV can be useful to screen for "anti-age" activity based on anti-oxidant or enzyme inhibitory activity, a more realistic approach to senescence study and slow-down is obtained with longer term cell culture studies involving proliferation rates, marker proteins and telomere analysis. Certain molecules are able to act on these mechanisms and lead to correlated *in vivo* activities.

[1] N Pineau, F Bernerd, A Cavezza *et al.* Eur J Dermatol 2008; 18 (1): 36-41
[2] Hayflick, L. (1985). *Clin Geriatr Med* **1**(1):15-27.

PAPILLARY DERMIS: A NEW BIOLOGICAL TARGET OF THE INTRINSIC CUTANEOUS AGING

David Boudier, Laetitia Marchand and Brigitte Closs

R&D Department, Silab, France

Introduction

The dermis is considered and recognized as the primary target of cosmetic products to combat skin aging. This macromolecular combination is composed of a diverse range of matrix molecules organized in a highly dynamic structure which has two dermal compartments separated by a vascular plexus: the papillary dermis and the reticular dermis.

Most recently, teams specialized in the study of the dermal matrix have focused their studies on the superior dermis in close contact with the Dermal Epidermal Junction (DEJ): the papillary dermis. This research activity is driven by the belief that this zone, a site of exchange and interaction, is a favorable target in intrinsic skin aging.

Indeed, early deterioration of the oxytalan fibers begins at 30-40 years: they gradually disappear under the DEJ until there are none left (1;2). The expression of collagens by papillary fibroblasts is also impaired. In consequence, the number and size of dermal papillae are reduced, a phenomenon reflecting the flattening of the DEJ (3;4).

Then, several scientific studies conducted on the papillary dermis showed that each type of molecules was related to a specific skin biomechanical property (5;6;7). With age, the skin loses some of its biomechanical properties, slackens and collapses. It is no longer capable of resisting stresses, and wrinkles appear.

Consequently, we developed an *in-vitro* model of intrinsic aging of the papillary dermis in order to study expression profiles of different matrix proteins.

Material and methods

Structural modifications of oxytalan fibers in young and mature skins

8 mm diameter punches were prepared from skin taken from both young and mature adult donors who had undergone cosmetic surgery. Explants were frozen and sections (4µm) were prepared with a cryostat. Selective staining of oxytalan fibers was realized as described (8).

Procedure used to obtain human fibroblasts from papillary dermis

Human papillary fibroblasts were retrieved using the same procedure as that by Sorrell's research team (9). They were isolated from adult donors who underwent plastic surgery. Using of a dermatome allowed us to control the cutting depth (0.2 – 0.3 mm). Human papillary fibroblasts obtained from four donors (average age 37 years) were mixed and cultivated.

In-vitro senescence of human papillary fibroblasts

Senescent human papillary fibroblasts were obtained by replication (30 passages).The *in-vitro* senescence of cells was monitored with the commonly used β-galactosidase staining in comparison with "normal" human papillary fibroblasts (8 passages).

Study by RTqPCR of expression of specific collagens XII and XVI and ubiquitous collagens VI and I

The study was carried out by Reverse Transcription quantitative Polymerase Chain Reaction (RTqPCR). After cells culture, total messenger Ribo Nucleic Acid (mRNA) was isolated. Following the standard reverse transcription of each RNA sample, the quantitative PCR analysis was performed.

Study by Western Blot of Fibrillin-1 synthesis on normal and senescent human papillary fibroblasts

After cells culture, supernatants were retrieved and deposited on a Sodium Dodecyl Sulfate-8% polyacrylamide gel. Proteins were then transferred to a membrane which was incubated with a primary murine monoclonal anti-fibrillin-1 antibody and a secondary HRP-coupled anti-murine IgG antibody. Peroxydase substrate and chromogen solution were used for visualization. Bands were semi-quantified by densitometry.

Results and Discussion

Structural modifications of oxytalan fibers in young and mature skins

Then, structure and organization of oxytalan fibers are modified with age. They become shorter, disorganized and lead to disappear.

In-vitro senescence of human papillary fibroblasts

Our *in-vitro* model of senescent papillary fibroblasts by replication was validated by visualization of the marker of senescence β-Galactosidase.

Study of expression of specific collagens XII and XVI and ubiquitous collagens I and VI
The RT quantitative PCR study clearly demonstrated that expression of collagens XII, XVI, I and VI was respectively and significantly reduced by 90%, 69%, 83% and 78%on senescent human papillary fibroblasts compared to normal. **Figure 1**

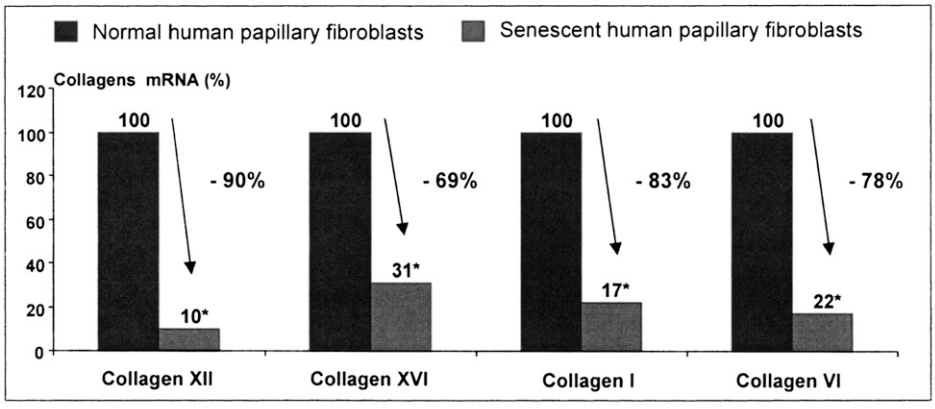

Figure 1: Expression profiles of collagens by normal and senescent human papillary fibroblasts

Study by Western Blot of Fibrillin-1 synthesis on normal and senescent human papillary fibroblasts
We confirmed modifications observed on skin sections by measuring the Fibrillin-1 synthesis, one of the main components of oxytalan fibers, which was significantly decreased by 31% on senescent human papillary fibroblasts compared to normal.

Conclusion
Recent studies showed that there was a close link between each collagen type and the architectural and functional characteristics of the papillary area: collagen XII is associated with deformability, collagen XVI with extensibility, collagen VI with cohesion and flexibility and collagen I with resistance of human dermis (10).
Thanks to this innovative approach of collagenic markers on an *in-vitro* model of intrinsic cutaneous aging of the papillary dermis, we were able to demonstrate a profound alteration of their expression profiles.
One interesting hypothesis is that the consequences of these modifications could be involved in the *in-vivo* intrinsic cutaneous aging process and similarly, in the appearance of wrinkles. We equally confirmed that Fibrillin-1 synthesis, one of the main components of oxytalan fibers, was decreased in our *in-vitro* model.
However, it has been observed that treatment with a *Cyperus esculentus* tuber extract leads to restore a normal expression profile of these different dermal markers. This gives us reason to believe that certain molecules would appear to have a direct effect on the papillary dermis, and can, therefore, retard the cutaneous aging process.

References
1. Pasquali-Ronchetti I, Baccarani-Contri M. *Microsc. Res. Tech*, **38**, 428-435 (*1997*).
2. Bouissou H, Pieraggi MT, Julian M, Savit T. *Int. journal of dermatology*, **27**, 5 : 327-334 (*1988*)
3. Sauermann K, Clemann S, Jaspers S, Gambichler T, Altmeyer P, Hoffmenn K, Ennen J. *Skin Research technology*, **8** : 52-56 (*2002*)
4. Asselineau D. Pageon H, Mine S. *J Soc Biol*. **202 (1)**, 7-14 (*2008*)
5. Kassner A, Tiedemann K, Notbohm H, Ludwig T, MÖrgelin M, Rheinhardt DP, Chu ML, Bruckner P, Grässel S. *J. Mol. Biol*, **339** : 835-853 (*2004*).
6. Ruggiero F, Roulet M, Bonod-Bidaud C. *J Soc Biol*, **199(4)** : 301-311 (*2005*).
7. Berthod F and al. *J. Invest. Dermatol*, **108** : 737-742 (*1997*).
8. Godeau G, Gonnord G, Jolivet O, Schoevaert D, Pompidou A, Lagrue G, Robert AM. *Anal Quant Cytol Histol.* **Dec;8(4)**: 321-5 (*1986*)
9. Sorrell JM, Baber MA, Caplan AI. *J. Cell. Physiol.*, **200**: 134-145 (*2004*).
10. Ruggiero F. Article in French. *Fc-3[Bio],* Lyon, (June *2007*).

COMPLYING WITH NEW FDA GUIDELINES FOR IN VITRO EVALUATION OF UVA PROTECTION

Olga V. Dueva-Koganov[1], Ph.D., Colleen Rocafort[1], Steven Orofino[1], Uli Osterwalder[2] and Juan Brito[1]

[1]CIBA Corporation, Tarrytown, New York
[2]CIBA Corporation, Basel, Switzerland

Introduction

There is an ongoing debate in the industry regarding various aspects of new FDA guidelines for assessing UVA protection of sunscreens *in vitro*. The purpose of this research is to establish *in vitro* test conditions for the evaluation of sunscreen UVA protection that closely follow the requirements published in the new FDA guidelines [1], and evaluate various sunscreens accordingly.

Method Description

Pre-irradiation criteria are fulfilled using a Ci65A Xenon Weather-O-Meter with Right Light™ inner/Quartz outer filter combination. This novel filter combination was recently introduced by Atlas [2] and provides an unparalleled match to natural sunlight especially in the UV region (Fig 1).

Spectral power distributions can be normalized to 1.57 W/m^2 or 1.1 W/m^2 at 420 nm allowing to reach 200 J/m^2 –erythemal effective dose (1 MED) calculated according to [1] within 10 or 14 min, respectively. Test articles with the same SPF values are irradiated simultaneously. Irradiation time is equal to SPF value of the test product multiplied by 2/3 and multiplied by the specific time to reach 1 MED. Application dose is 2 mg/cm^2. Substrate Vitro Skin® N-19 [3] is utilized as a suitable alternative for roughened quartz plates due to the following reasons: Vitro Skin® works well with applications dose recommended by FDA and spot to spot variability in substrate's own transmittance is low; currently there is no commercial source for roughened quartz plates with standardized roughness; quartz substrate roughness is not specified in the FDA guidelines, however it was shown by Louis Ferrero *et al* [4] that this parameter is important for reproducible measurements; 2 mg/cm^2 dose applied on roughened quartz substrate creates technical problems with measurements of transmittance values, especially for sunscreens with SPF 50+.

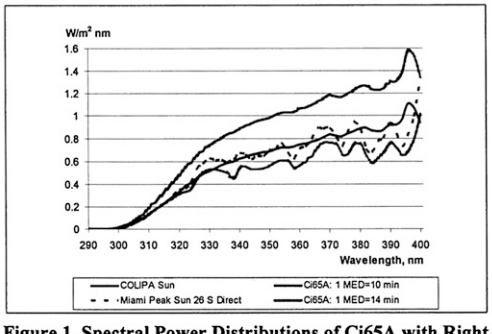

Substrate is pre-cut into 6.5 cm x 6.5 cm pieces and pre-hydrated according to [3]. This substrate size provides sufficient area to conduct the transmittance measurements of 12 different locations. Substrate is placed in a slide mount and used as a reference. Sunscreen is applied on the substrate and placed in a similar slide mount.

Application time is increased to 30 sec because 10 sec recommended in [1] are not enough to achieve uniform distribution over the substrate on a relatively large application area, especially if the test article contains particulates.

Figure 1. Spectral Power Distributions of Ci65A with Right Light™ inner/Quartz outer filters normalized at 420 nm to 1.57 W/sq.m^2 and 1.1 W/m^2; COLIPA Sun and Miami Peak Sun 26S Direct

Slides with reference sample without sunscreen (C) and the sample with applied sunscreen (P) are placed in the sample holders and irradiated in Ci65A Xenon Weather-O-Meter. After pre-irradiation, the measurements of transmittance (T) are conducted using Optometrics SPF 290S with wavelength step of 5 nm. A minimum of 12 measurements of spectral irradiance transmitted through the reference ($C(\lambda)_1 \ldots C(\lambda)_{12}$) and with applied sunscreen product ($P(\lambda)_1 \ldots P(\lambda)_{12}$) are required to calculate the mean transmittance value at each wavelength and its standard deviation s:

$$\overline{T(\lambda)} = \frac{\sum_1^n P(\lambda)/n}{\sum_1^n C(\lambda)/n} \qquad s = \sqrt{\left[\frac{\overline{P(\lambda)} \times s(C(\lambda))}{(C(\lambda))^2}\right] + \left[\frac{s(P(\lambda))}{C(\lambda)}\right]^2}$$

The standard deviation is evaluated using Taylor's approximation, and it requires calculations of the standard deviation of the measurements of $C(\lambda)$ and $P(\lambda)$:

$$s(C(\lambda)) = \sqrt{\frac{\sum_1^n \left(C(\lambda) - \overline{C(\lambda)}\right)^2}{(n-1)}} \qquad s(P(\lambda)) = \sqrt{\frac{\sum_1^n \left(P(\lambda) - \overline{P(\lambda)}\right)^2}{(n-1)}}$$

This calculation generates 23 transmittance values with associated standard deviations, one for each 5 nm wavelength increment from 290 to 400 nm. The coefficient of variation, which is the standard deviation divided by the mean and expressed as a percentage, provides an indication of the uniformity of the sunscreen layer; this value should be less than 10%. At least five repetitions are used for each test article. In some instances, more than 5 repetitions are needed to meet the coefficient of variance requirement.

To determine UVA1/UV ratio and UVA rating category, which could be low (0.20 to 0.39), medium (0.40 to 0.69), high (0.70 to 0.95) or highest (greater than 0.95) - the following calculations are needed. Spectral transmittance values T are converted into absorbance values A. The index of UVA protection is calculated as the area per unit wavelength under portions of a plot of wavelength versus $A(\lambda)$, divided by the area per unit wavelength under the total curve. UVA I area per unit λ is:

$\int_{340}^{400} A(\lambda)H(\lambda)B(\lambda) \Big/ \int_{340}^{400} d(\lambda)$, and UV area per unit λ is $\int_{290}^{400} A(\lambda)H(\lambda)B(\lambda) \Big/ \int_{290}^{400} d(\lambda)$

The integrals in these formulas are evaluated using Simpson's rule for irregular areas, and $B(\lambda)$ – action spectrum factor is equal to 1 for all wavelengths [1].

Experimental Results and Discussion

Test articles - several commercial and experimental products (marked by *) containing various sunscreen actives are presented in Table 1, and their transmittance values after irradiation versus wavelength are shown in Fig. 2.

Table 1. Test articles and their respective UVA1/UV ratios

	A SPF15	B* SPF20	C SPF15	D SPF15	E SPF30	F* SPF30	G* SPF50
ACTIVES	CONCENTRATION OF ACTIVES, %						
Avobenzone	3	2.7		2	3	3	3
Octocrylene	10	9			2.35	2.5	5
Homosalate				10	8		
Octisalate				5	4		
Oxybenzone			5	3	5		
Octinoxate			7.5				
Bemotrizinol						3	2
Bisoctrizole		5				2.5	5
Dose, MED	*10*	*13.3*	*10*	*10*	*20*	*20*	*33.3*
UVA1/UV Ratio - range	0.857-0.880	0.913-0.939	0.441-0.475	0.727-0.753	0.809-0.830	0.914-0.930	0.951-0.960

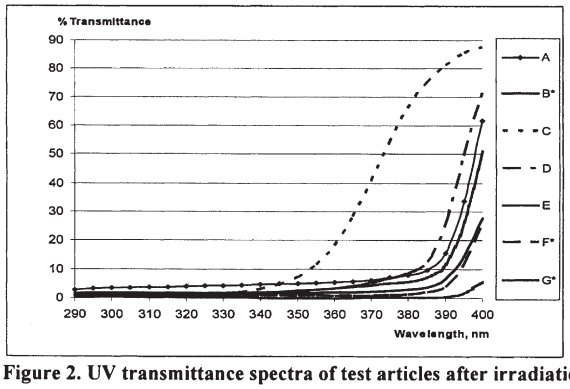

Figure 2. UV transmittance spectra of test articles after irradiation

A majority of the commercial sunscreens tested belong to medium or high UVA protection categories (Table 1).

Test article G* containing broad-spectrum actives bisoctrizole and bemotrizinol in conjunction with avobenzone and octocrylene achieved the highest UVA rating category.

The addition of bisoctrizole to the combination of avobenzone and octocrylene improves UVA1/UV ratio – based on the data obtained for test articles A and B*.

Conclusions

The optimal test conditions, which closely follow the requirements published in the new FDA guidelines for the *in vitro* evaluation of UVA ratings were established and successfully utilized for the evaluation of several commercial and experimental sunscreen products.

It was demonstrated that it is possible to meet the highest UVA rating requirement by optimizing the composition of sunscreen actives and assuring the photostability of the product.

References

1. Federal Register, 21 CFR Parts 347 and 352 Sunscreen Drug Products for Over-the-Counter Human Use; Proposed Amendment of Final Monograph; Proposed Rule, **72(165)**, 49070-49122, §352.71 *(2007)*

2. Atlas SunSpots® *Material Testing Product and Technology News* **38(81)**, 14-15 *(2008)*

3. http://www.ims-usa.com/ittrium/visit?path=A1x66x1y1xa0x1x65y1xc6x1x65y1xccx1x65

4. Louis Ferrero, Marc Pissavini, Stephanie Marguerie and Leonhard Zastrow *International FSCC Magazine*, **Vol 7(3),** 197-205 *(2004)*

Acknowledgements

We are very grateful for the support of our colleagues at Ciba, especially Dr. Joseph Lupia, Dr. B. Scott Jaynes, Gustavo Vazquez, Shawn O'Brian and Shiela Loggins.

A NOVEL EX VIVO PIG SKIN ORGAN CULTURE MODEL FOR USE IN EFFICACY AND SAFETY TESTING

Gabriele Vielhaber[1], Ph.D., Michele Massironi[2], Ph.D. and Paolo Pertile[2], Ph.D.

[1]*Symrise GmbH & Co KG, 37603 Holzminden, Germany*
[2]*Cutech Srl, 35127 Padua, Italy*

Introduction

The efficacy and safety requirements for cosmetic products are continuously increasing while the use of animals for testing cosmetic ingredients has been banned by the 7th amendment of the EU cosmetics guidelines. We therefore developed a novel ex vivo skin model with an extended viability and functionality. We chose pig skin as the morphological and functional features of the pig's skin and hair follicles strongly resemble human skin, while showing a much lower inter-individual variability and can be used without ethical concerns. As the pig skin derives exclusively from slaughter material, its use is not considered as animal testing.

Methodology

Skin from dorsal areas of pietrain hybrid pig was resected, cut into 4x4x3 mm pieces (WxDxH) and placed in culture at the air-liquid interface on a sterilized cotton pad soaked with 5 ml of customized DMEM. The culture medium was replaced every 3 days. Assays were started 24 h after sample acclimatization at 37°C, 5% CO_2. Hair growth was tested by quantifying the number of proliferating, Ki67 positive hair matrix cells. Skin irritation was measured with methyl green pyronine staining according to Jacobs et al. [1]. For sensitization testing, the number of CD1+ positive cells (i.e. Langerhans cells) that migrated from the epidermal layer to the dermis was determined by immunohistochemistry.

Results and Discussion

Hair follicle density was found to be fundamental to skin preservation, as samples with lower hair follicle densities contained fewer proliferating cells (Table 1). The hair follicles were fully and significantly responsive for up to day 21 of culture to modulators of hair growth as cyclosporine A (stimulator) and TGFß2 (inhibitor) (not shown).

	Day 0		Day 6	
Sample	A	B	A	B
Hair follicle density (No./cm^2)	30 ± 5	11 ± 3	30 ± 5	11 ± 3
% of Ki-67-positive cells	5.37 ± 0.76	2.74 ± 0.37	4.03 ± 0.20	0.98 ± 0.05
% proliferation vs. A, day 0	100	51	75	18

Table 1: Number of proliferating cells versus hair follicle density at day 0 and day 6 of PSOCM culture

We further tested the suitability of the PSOCM for evaluating irritants and sensitizers by using sodium dodecyl sulfate (SDS) and nonanoic acid as classic irritants and 2,4-dinitrochlorobenzene (DNCB) and cinnamic aldehyde (CIN) as benchmark sensitizers. Cytotoxicity is considered to be the first and major trigger of skin irritation. We therefore determined first the highest non-irritant concentration for the test compound by measurement of keratinocyte viability by methyl green pyronine (MGP) staining. A concentration with a MGP score of ≤ 0.35 was considered as irritant. The compounds were further assessed for their sensitizing potential by analyzing the number of Langerhans cells (LCs) (CD1a-positive) that migrated from the epidermal layer to the dermis as a consequence of an immunoreaction [2]. The test compound was considered as sensitizing when the percentage of migrating LCs was significantly higher than in the control vehicle at non-irritant concentrations.

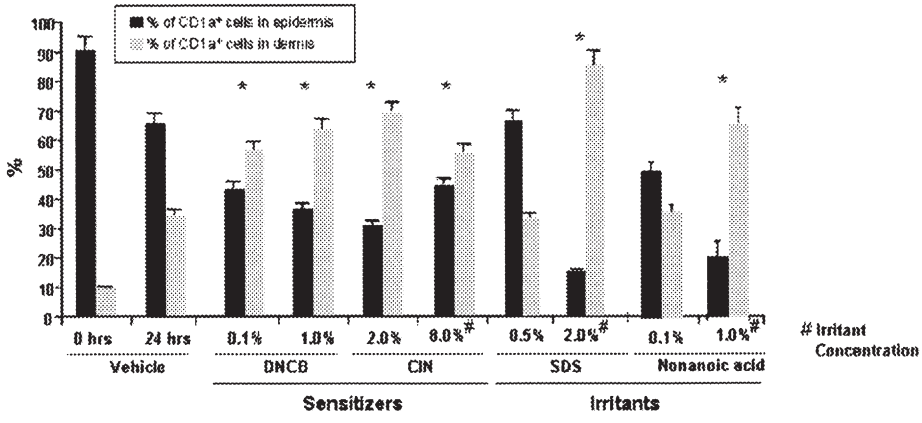

Figure 2: Induction of Langerhans cell migration by sensitizers and irritants. Percentage of CD1+ cells in the epidermis and dermis, respectively after 24h incubation. * $p<0.05$ vs. vehicle.

All ingredients showed the expected reaction, as the irritants reduced the skin samples' viability, without inducing LC migration at non-irritant concentrations and the sensitizers significantly activated Langerhans cell migration at non-irritant concentrations (Figure 2). Moreover, the ex vivo pig skin model was sucessfully used for efficacy testing of skin lighteners, anti-aging and lipolytic ingredients.

Conclusions

We conclude that the PSOCM is an ethical, versatile, and economical alternative to animal testing. It shows reliable biological responsiveness for up to 21 days of culture, thus enabling long-term experiments. It is suitable for testing the efficacy of a variety cosmetic ingredients as e.g. modulators of hair growth, skin lighteners, anti-aging and lipolytic ingredients. The results obtained in assessing skin irritation and skin sensitization are very promising, but need further validation. We are continuing the testing with special emphasis on the assessment of fragrance materials.

References

[1] Jacobs JJL, Lehe C, Cammans KDA, Das PK, Elliott GR *ATLA* **28**, 279-292 (*2000*)

[2] Jacobs JJL, Lehe C, Cammans KDA, Das PK, Elliott GR *Toxicol. in Vitro* **18**, 681-690(*2004*)

MULTIFUNCTIONAL SHINE AND HOLD TECHNOLOGY FOR ETHNIC HAIR CARE

Andrea Keenan, Robert Antrim, Ph.D. and John Reffner, Ph.D.

Rohm & Haas Company, Spring House, PA

Introduction:
Hair shine has long been sought after by consumers in the ethnic hair care market and many researchers have attempted to quantify the luster. Typically formulators turned to silicone based products, contributing qualities such as shine, conditioning, repairing and minimizing the effects of heat and chemical treatments [1, 2, 3]. There are areas that the silicone based technology has some limitations such as all day hold, stylability, and humidity resistance. In this study we will demonstrate that hair fixative polymer technology like acrylates/hydoxyesters acrylates copolymer can enhance shine on ethnic hair and other types of hair, providing style retention and humidity resistance, without weighing hair down. These polymers add luster to the consumer's hair due to their inherent film formation properties; their film coverage is a distinctive balance between viscosity, surface tension and film adhesion, which results in a smooth, uniform surface across a hair shaft.

Methodology:
Instrumental measurements using the Bossa Nova Samba video camera with the specular and diffuse reflectance were used to quantify the luster on hair shafts treated with acrylate based polymeric film formers [4, 8]. Confirmatory studies were completed utilizing atomic force microscopy to show improved smoothness along the hair shaft due to polymer spreadability and uniformity [5, 6, 7, 9]. Additional analytical techniques were used to complement our luster findings; including surface tension analysis and refractive index measurements. Panel tests were carried out to determine whether the panelist's visual assessment corresponded with the instrumental results.

Results:
Averages of 5 untreated hair swatches were analyzed using the Bossa Nova Samba Shine Instrument. Tresses were then treated with an alcoholic solution of copolymers, dried and the hair tresses were reanalyzed. Included as a control, was a commercially available silicone based shine spray. Hair types included in this study: Kinky African, Latin, Asian and Caucasian Hair. The chart illustrates the enhanced shine delivered from the acrylates/hydroxyesters acrylates copolymers 1 or 2 compared to the silicone containing spray on Kinky African Hair. Irregardless of the equation used to calculate luster, Reich Robbins, TRI Method or Bossa Nova Technologies, the acrylates based copolymers are equal or better than the silicone treatment for hair luster. See Figure 1.

Equations

Reich Robbins: $100*S/(D*\theta_o)$ TRI Method: $100*S/(S+D)*\theta_{ref}/\theta_0$ Bossa Nova: $100*S_{in}/(D+S_{out})+W_{visual}$

Atomic Force Microscopy has been commonly used for characterization of topographical and mechanical properties of surfaces by use of a mechanical probe sensing the surface, in this case for roughness. The evaluations were performed on single untreated hair fibers. The fibers were then treated with alcoholic solution of copolymers, air dried, then re-imaged for changes or improvements in the surface roughness. The **Z** value is measured as the depth from peak to valley along the length of the hair shaft. **Ra** is measured as the surface roughness or surface topography. **Ra** can be interpreted as a sensing of the overall surface, taking into consideration the variability in height along the hair shaft as the tip of the probe is traversing along the surface. The Delta **Z** or **Ra** = Pre-treatment – Post treatment, where a *Higher number = Smoother surface = Higher shine*. The AFM results reveal the concept of surface effects by illustrating the polymers ability to spread on the hair shaft to create a smooth surface topography. See Figures 2-4 and Table 1.

Table 1

Hair Type	Treatment	Delta Z	Delta Ra	Hair Type	Treatment	Delta Z	Delta Ra
Latin	AHEAC 1	844	61	Asian	AHEAC 1	12	5
Latin	Silicone	52	3.5	Asian	Silicone	11	0
Latin	AHEAC 2	827	108	Asian	AHEAC 2	0	0
Kinky	AHEAC 1	129	0	Caucasian	AHEAC 1	443	87
Kinky	AHEAC 2	935	66	Caucasian	AHEAC 2	343	35

* AHEAC = Acrylates/Hydroxyesters Acrylates Copolymer

Panel tests were carried out to determine whether the panelist assessment corresponded with the instrumental results. Hair Tresses were evaluated in a black box, scale 1-5, 1=matte 5= high gloss. Panelists invariably chose the hair swatches treated with the acrylate based polymer as having more luster than the hair swatches with the silicone treatment. The instrumental measurements and the analytical techniques demonstrated very good correlation with the evaluations from the panelists indicating improvements in hair luster using acrylate based polymers. See Figure 5.

Hair tresses were curled, and then treated with the AHEAC 1 and 2 and with the control silicone spray. The tresses were dried, and then exposed to a High Humidity Chamber for 8 hrs at 90% Relative Humidity and 30°C. The acrylates/hydroxyesters acrylates copolymers were able to maintain their style retention and control while the silicone containing product had significant loss in style control under humid conditions.

Conclusions:

Results indicate hair luster can be enhanced, on ethnic hair as well as other hair types, with the use of acrylates/hydroxyesters acrylates copolymers. The acrylate copolymers uniquely deliver a discernable shine as well as strong hold and all day style control.

References:

1. M. Starch, Cosmetic & Toiletries **114**, 55-60 (1999)
2. C Reich and CR Robbins, J Soc Cosmet Chem **44,** 221-234 (1993)
3. I. Reeth, M. Starch, J. Decaire, Dow Corning Corp, (2000)
4. J. Lim, M. Chang, M. Park, J Cosmet Sci **57**, 475-485 (2006)
5. N. Starostina, M. Brodsky, S. Prikhodko, J Cosmet Sci **59**, 225-232 (2008)
6. B. Bhushan, G. Wei, P. Torgeson, Ultramicroscopy **105**, 248-266, (2005)
7. B. Bhushan, C. LaTorre, Ultramicroscopy **105**, 155-175 (2005)
8. N. Lechocinski, P. Clémenceau, Bossa Nova Technologies, LLC (2007)
9. B. Bhushan, H. Fuchs, C. LaTorre, Applied Scanning Probe Methods IV, 35-103 (2006)

Figure 1

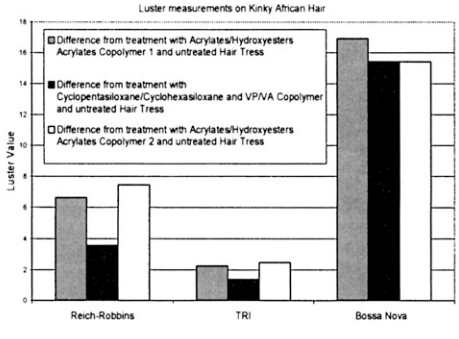

Figure 5

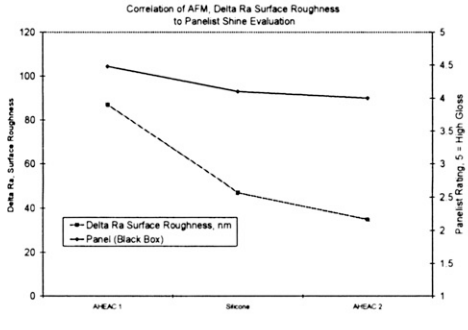

Figure 2-4
Single hair shaft treated with

AHEAC* 1 Silicone AHEAC 2

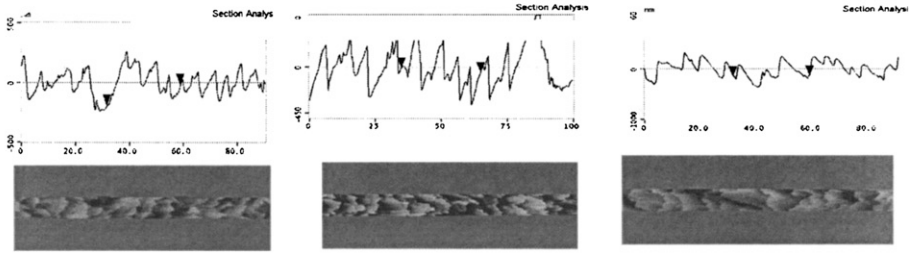

WATER- AND SWEAT-RESISTANT STYLING USING ACRYLATE POLYMERS

Duane G. Krzysik[1], David Faivre[2], Dorina Ghirardi[2], Mariam Mouedden[2] and Marie Ollagnier[2]

[1]*Lubrizol Advanced Materials, Noveon Consumer Specialties, Cleveland, Ohio*
[2]*Lubrizol Advanced Materials, Noveon Consumer Specialties, Brussels, Belgium*

Introduction
The heaviest users of styling products are typically young, highly social consumers leading active lifestyles. A single day's activities might include sports, weight training and other aerobic exercise, a full day of work or school, shopping, commuting, dining, and perhaps all topped off by a visit to the café or dance club to socialize with friends. This dynamic, 24/7 lifestyle puts incredible demands on the styling products used by these consumers, leading them to seek and appreciate product claims such as "water-resistant" and "sweat-resistant".

It is well known that the performance of styling products formulated with traditional fixatives are negatively impacted by moisture from sources including inclement weather, environmental humidity and human sweat. Because of their hygroscopic nature, these traditional fixatives show high sensitivity to moisture, which leads to film tackiness and a loss in holding power in these challenging conditions. Overcoming this performance gap is an important challenge facing formulators.

Objectives
In this study, the water resistance of the film-forming fixative polymers polyacrylate-14, polyacrylate-2 crosspolymer and acrylates copolymer and combinations of these polymers were investigated. Another objective of this work was to investigate the formulations' physical properties (viscosity, yield value and clarity) as well as other fixative performance properties.

Methods
The water/sweat resistance on hair was conducted using the Water/Sweat Resistance Style Retention Method. In this method 2.5g European virgin brown hair tresses are washed with a 10 wt% total solids sodium laureth sulfate solution. The tresses are dosed with 0.35 – 0.40g of test formulation and are laid flat between two perforated Teflon® coated plates and allowed to dry overnight at 50% relative humidity and 25°C. The next day the dried, treated hair tresses are gently removed from the coated plates and suspended in a beaker of 25°C artificial sweat water for 5 seconds. The composition of the artificial sweat water is 0.20 wt% total solids solution of NaCl (1,200mg), MgSO4 (36mg) and KCl (300mg) adjusted to a pH of 5.5 with lactic acid. After immersion in the artificial sweat water, the tresses are then clamped at a 45° angle on a curl retention board and the initial point is recorded. A hair tress is considered to have failed when it displays less than 70% retention after 15 minutes.

The equation for Percent Curl Retention is:

$$\frac{\text{Length of Uncurled (Straight) Hair Tress} - \text{Length of Curled Hair Tress at Time of Reading}}{\text{Length of Uncurled (Straight) Hair Tress} - \text{Length of Curled Hair Tress at Start of Test}} \times 100 = \%\ \text{Style Retention}$$

Multiple tresses are evaluated and the results are reported as an average of the tresses tested. Results are compared between formulations.

Viscosity, yield value and clarity of the formulations tested were measured and recorded. In addition, both mechanical stiffness and high humidity curl retention were conducted to determine the other fixative benefits of the formulations tested.

Results
Study 1: Individual Polymers
Polyacrylate-14, polyacrylate-2 crosspolymer and acrylates copolymer were evaluated at different solids levels to determine their water/sweat resistance using the basic formulation of water and polymer at the different test concentrations adjusted to a pH of 7.0 – 7.3. Only one polymer, polyacrylate-2 crosspolymer was able to provide water resistance when used alone.

Polyacrylate-14 (wt% total solids)	Polyacrylate-2 Crosspolymer (wt% total solids)	Acrylates Copolymer (wt% total solids)	Water / Sweat Resistance
1.0			< 70 %
2.0			< 70 %
	2.5		85 %
	3.0		85 %
		1.2	< 70 %
		2.0	< 70 %

Study 2: Combination of Polymers

Polyacrylate-14, polyacrylate-2 crosspolymer and acrylates copolymer were evaluated in various combinations and at different solid levels to determine their water/sweat resistance using the basic formulation of water and polymer combinations at the different test concentrations adjusted to a pH of 7.0 – 7.3. Combinations of acrylate polymers were found to provide water/sweat-resistance. The combinations of polyacrylate-14 and acrylates copolymer provide synergistic water/sweat-resistance.

Polyacrylate-14 (wt% total solids)	Polyacrylate-2 Crosspolymer (wt% total solids)	Acrylates Copolymer (wt% total solids)	Water / Sweat Resistance
1.0	2.5		86.9 %
1.0		1.2	91.3 %
	2.5	1.2	86.9 %
2.0	1.0		85.0 %
3.0	2.0		87.0 %
2.0		1.0	85.0 %
3.0		2.0	86.0 %

Results of Benefit Testing

Combinations of these polymers also provide excellent levels of stiffness and high humidity curl retention using the spiral curl method.

Conclusions

Polyacrylate-2 crosspolymer alone or in combination with acrylate polymers provides water/sweat-resistance. There also appears to be a synergistic water/sweat resistance effect from a combination of polyacrylate-14 and acrylates copolymer. Therefore, through the use of specialized hydrophobically modified acrylate film-forming polymers, the water/sweat-resistance properties of styling formulations can be improved to better meet the needs of these demanding consumers.

MEASUREMENT OF HAIR MOISTURE CONTENT UTILIZING NOVEL ANALYTICAL AND REAL-TIME TECHNIQUES

Michael G. Davis and Sam W. Stofel

P&G Beauty, Sharon Woods Innovation Center, Cincinnati, Ohio 45241

Background

Consumers have long sought "moisturized" hair and are drawn to hair care products that claim to provide this benefit. We and others have strived for many years to provide the best technical measure for this consumer desire. In the literature there exist many technical reports describing the use of analytical techniques to accurately measure water/moisture in the hair. In the interest of continuing to improve our technical knowledge regarding this desire, we have measured the sensory perception of moisturized hair and compared it with novel technical measures for environmental moisture and hair moisture content.

Methods

Sensory: In this study, we merged sensory techniques with instrumental measurements to describe a woman's moisture environment. To accomplish this, we have used panelists trained to feel differences between hair treatment products. They were asked, in a double-blinded fashion, and without visual cues, questions regarding the tactile properties of prepared hair switches. All hair switches used were equilibrated for 48 hrs at described constant temperature/constant relative humidity rooms and sensory measures were made under constant temperature/constant relative humidity.

Moisture Measurements: In order to accurately determine the moisture content at the time of perception, we have re-applied a novel microwave resonance measurement to hair. This was accomplished using the MW3150 MoistureWave® device coupled with a 13mm cylindrical sensor chamber from TEWS Elektronik (Hamburg, Germany). We have previously described validation and the use of this instrument for hair applications (Textile Research Institute, Hair 2008 poster session).

Real Time Environmental Monitoring was accomplished using TK500 portable humidity and temperature dataloggers from Dickson Instruments (Addison, Illinois USA). Panelists were told to wear the devices for 24hrs and proceed through their day as normal. Monitoring was performed in fall, winter and summer months in the Cincinnati, Ohio area. Upon return, the data from the monitors was downloaded using the supplied communication software and graphed.

Results

We explored the consumer's perception of the term "moisturized" in a series of sensory experiments. In order to determine if the term "moisturized" was dependent upon the tactile properties of the hair we first provided panelists with switches equilibrated at 45% relative humidity (RH) that were either purposefully tangled or combed straight. As can be seen in Figure 1a, the sensory data indicates that panelists chose the untangled switches as being not only smoother but also more "moisturized" despite the fact that there was no difference in the moisture, or water, content in the hair as determined by microwave resonance. In a second experiment, we changed the equilibration humidity to either 15%RH or 80%RH and asked panelists to evaluate switches when brought together at 45%RH. Figure 1b shows that panelists perceive the switches initially equilibrated to 15%RH to be more "moisturized" than those equilibrated to 80%RH even though microwave resonance confirms that the 80%RH switches have significantly higher moisture content at the time of evaluation. We hypothesize that this could also be dependent upon the bulk properties of the hair due to the fact that the switches equilibrated at 80%RH had also become "frizzy".

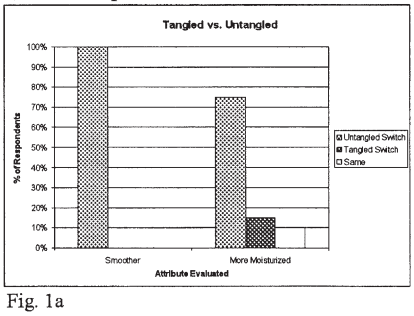

Fig. 1a

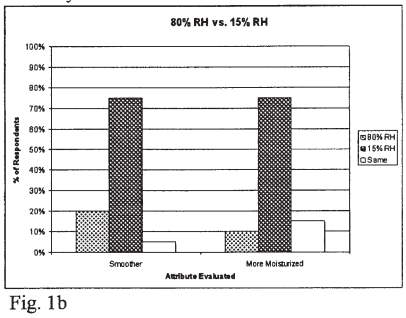

Fig. 1b

In the interest of determining the actual environment surrounding a consumer throughout the day we used the dataloggers to map the temperature and RH changes that a consumer may experience in a single day. Figure 2a shows a representative sample of the real-time atmospheric moisture and temperature measurements. This chart shows the constant fluctuations in temperature and relative humidity throughout a 24 hour period day with no apparent "steady state" achieved except while sleeping. This observation combined with readings from the microwave resonance data on hair switches showing that it can take up to 12 hours for a hair to fully equilibrate to its environment (Fig. 2b), implies that constant environmental fluctuations might not permit hair to reach an equilibrium state

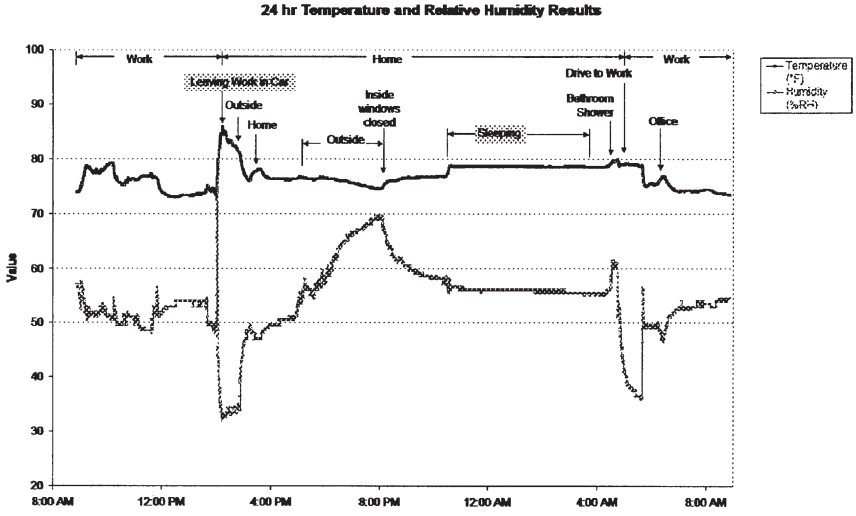

Figure 2a

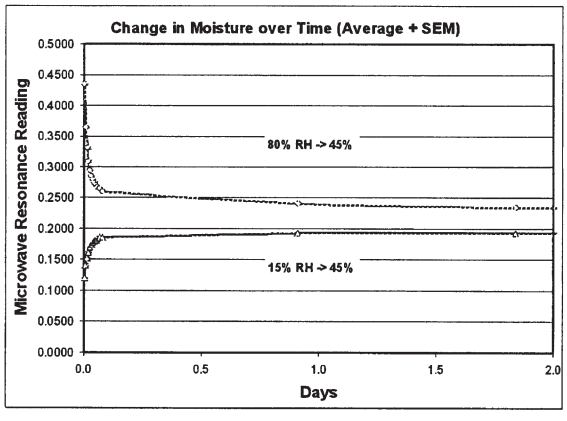

Figure 2b

Conclusions

In this paper we have shown data to suggest no correlation between the moisture content of the switch and the positive sensation of "moisturization" as it relates to hair but rather a correlation between "moisturization" and smoothness or softness. We have also shown data to imply that constant environmental fluctuations might not permit hair to reach an equilibrium state.

It is our hypothesis that by investigating the true definition of women's desire for "moisturized" hair we enable hair scientists to find common ground on the meaning of "moisturized" hair and women to better understand how to achieve the desired hair feel.

SMALL ANGLE NEUTRON SCATTERING STUDIES OF HUMAN HAIR: RELEVANCE TO DISTRIBUTION OF WATER

Yash Kamath[1], Ph.D. and N. Sanjeeva Murthy[2]

[1]*Kamath Consulting, Inc.*
[2]*Center for Biomaterials, Rutgers University*

Introduction

Human hair, being a protein fiber, is very sensitive to the presence of moisture. The mechanical properties of hair, such as tensile strength, bending and torsional rigidity are sensitively dependent on the amount of water in the fiber. It is also known that the amount of water in the fiber depends on the relative humidity of the environment. The fiber equilibrates, rather slowly, to the changes in the amount of moisture in the environment. This behavior has been studied and quantified in detail, using dynamic vapor sorption analyzer [1]. This apparatus determines the amount of water absorbed by hair gravimetrically from moisture vapor surrounding the hair sample at a given relative humidity (RH). From the data, a sorption isotherm is generated by plotting the water uptake against RH%. A sorption isotherm gives information about the water held in hair in different forms at varying RHs. For example, up to ~20%RH water is held in the form of a monolayer, from ~20-65% in the form of multi molecular layers and above 65% in the form of free water held in relatively large pores (capillary condensation). Water held by capillary condensation leads to swelling of the fiber.

An alternate method to study the distribution of water in hair could be small angle neutron scattering. To achieve this, the water in the sample is exchanged for heavy water (D_2O) and the resulting neutron-scattering contrast can be used to follow the structural changes that occur upon hydration. Such work has been done by Murthy et al. on synthetic polyamide nylon 6 [2]. We were interested to see what kind of information can be obtained from such measurement about the structure of hair and the distribution of water.

Experimental

The neutron scattering experiments were carried out on European dark-brown hair. Hair was aligned in the form of a thin tress (~0.5 mm in thickness) and 20mm in width were mounted on U-frames made of aluminum plate using superglue. These plates were placed in an airtight cell to maintain proper humidity conditions. We selected three different humidities (33, 75 and 95% RH) for this study. These humidity levels were obtained with saturated solutions of calcium chloride, sodium chloride and sodium sulfate in D_2O, respectively. The hair samples were kept under vacuum for 24 h to remove water. The samples were subsequently equilibrated for several days in the presence of saturated salt solutions with D_2O before exposing them to the neutron beam. Another set of samples were prepared by equilibrating them first at the desired humidity for 24 h and then keeping the sample under vacuum at room temperature to remove free D_2O. A wet sample was also included in the study. The equilibrated samples were placed between quartz plates and exposed to the neutron beam. The data were normalized to tress thickness.

Results and Discussion

Two dimensional distribution of intensity of scattered neutrons is shown in **Figure 1a**. In the figure the arrow indicates the orientation of the alignment of fiber axes. From the two dimensional distribution we can get a one dimensional intensity scan perpendicular to the fiber axes. This is plotted in **Figure 1b** as a function of q, where q is given by

$$q = 4\pi \sin\theta / \lambda$$

The spacing between the scattering entities is calculated by Bragg's equation

$$d = 2\pi / q$$

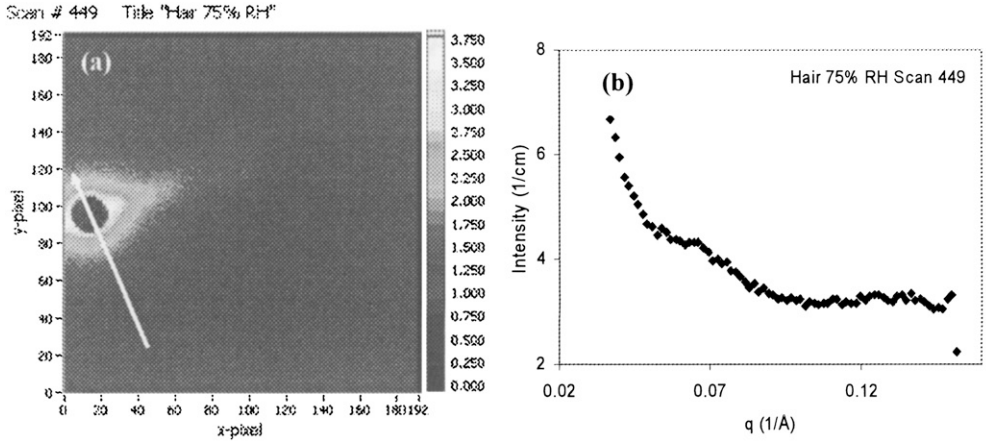

Figure 1. (a) Two dimensional map of intensity of scattered neutrons. Side bar shows the intensity level. The round spot is the beam stop with zero intensity. (b) One dimensional neutron intensity scan as a function of the scattering angle. We see a shoulder at q = 0.07 and a minor peak at q = 0.13. d values corresponding to these are 9.5 and 4.8 nm, respectively.

The neutron intensity map in Fig.1a shows that most of the water is present in macropores (scattering near the beam stop) and relatively small quantity of heavy water (less than 1 %) is probably present in the matrix between the intermediate filaments (weak lobe of intensity on the equator). This d-spacing, calculated from the peak at q = 0.07 $Å^{-1}$ in Fig. 1b, is 95 Å. The size of the intermediate filament is given to be ~7.5 nm. There also appears to be a structure with a spacing of 48 Å (q ~ 0.13 $Å^{-1}$) that may correspond to the heavy water between the protofilaments constituting the intermediate filaments. An important observation in this study was that the scattering pattern corresponding to q =0.07 and 0.13 was independent of the amount of water in the sample. This suggests that this small amount of water is strongly adsorbed or even exchanged between the amide functionality of the protein. This was observed even with samples evacuated after equilibration with heavy water. It is possible that an exchange of the following type takes place.

$$2\ CO\text{-}NH + D_2O \Rightarrow 2\ CO\text{-}ND + H_2O$$

This has been observed by Murthy et al. in the case of nylon by FTIR studies of the deuterated sample.

Conclusions

This preliminary study of the small angle neutron scattering of human hair has shown that water is present in essentially two forms. One which is adsorbed through hydrogen bonding and exchanged with amide nitrogen, and the other in macroporous regions. Neutron scattering cannot distinguish gradations in the latter. Results of additional experiments will be included in the final presentation.

References

1) "Effect of Oil Films on Moisture Vapor Absorption on Human Hair", J. Cosmet. Sci.,Karen Keis, Craig L. Huemmer and Y. K. Kamath, 58, 135-145 (2007).
2) "Structural Changes Accompanying Hydration in Nylon 6", Macromolecules, N. S. Murthy, M. Stamm, J. P. Sibilia and S. Krimm, 22, 1261-1267 (1989).